Appl Phys B (2011) 103:841–846
DOI 10.1007/s00340-010-4293-2

Applied Physics B
Lasers and Optics

Controlling number of lasing modes for designing short-cavity self-mode-locked Nd-doped vanadate lasers

Y.F. Chen · Y.J. Huang · P.Y. Chiang · Y.C. Lin · H.C. Liang

Received: 12 August 2010 / Revised version: 30 September 2010 / Published online: 23 November 2010

Abstract A short-cavity Nd:YVO_4 laser is employed to confirm that a spontaneous mode locking (SML) typically occurs without employing an extra nonlinearity. We further experimentally demonstrate that reducing the number of longitudinal lasing modes can diminish the phase fluctuation and effectively improve the SML pulse stability. Considering the spatial hole-burning (SHB) effect, an analytical expression is derived to accurately estimate the number of longitudinal lasing modes for a practical design guideline.

1 Introduction

The appearance of spontaneous mode locking (SML) in laser cavity without using additional nonlinearity except gain medium is an intriguing phenomenon of laser emission. During the early research on mode-locking, the SML phenomenon was observed on different types of lasers including He–Ne [1], ruby [2], Nd:glass [3], and argon ion [4] laser systems. In the mid-1960s, the SML was not considered to be a reliable approach for the generation of ultrashort pulses, partly because the mechanism for SML was not adequately understood. Recently, fairly stable SML pulses have been obtained in the experiments of Nd-doped vanadate miniature lasers [5] and Nd-doped double clad fiber lasers [6]. With the statistical analysis it has been shown that unless a systematic phase fluctuation over 2π is introduced, the mode-locked behavior will always be observed in a multimode laser [7, 8]. Although a systematic phase fluctuation is usually caused by dispersion effects, theoretical studies on the SML mechanism have confirmed that the combination tones of the third order nonlinear polarization terms can help in compensating the dispersion-induced phase shift [6, 9, 10]. As a result, the SML typically occurs in a multimode laser without employing an extra nonlinearity except the gain medium. However, the locking strength due to the nonlinear polarization terms is rather insubstantial. It is therefore crucial to precisely control the number of lasing modes for achieving relatively stable SML pulses.

Spatial hole burning (SHB) in the gain medium has been confirmed to be advantageously utilized for lasing mode selection [11–16]. In this work we first experimentally confirm that the separation between the gain medium and the end mirror in a standing-wave SML laser cavity can be employed to precisely control the number of longitudinal lasing modes via the SHB effect, leading to a stability improvement of the mode-locked pulses. With mode-locked states as a basis, we derive an analytical formula to analyze the number of longitudinal lasing modes. The predictions of the theoretical model have shown a fairly good agreement with experimental results.

2 Experimental results

We recently demonstrated that the large third-order nonlinearity of Nd-doped vanadate crystals could be used to achieve a short-cavity SML operation [5]. Here we employ the Nd:YVO_4 crystal to explore the influence of the number of longitudinal lasing modes on the stability of the SML performance. The cavity configuration is a linear concave-plano resonator, as shown in Fig. 1(a). The separation between the laser crystal and the input mirror, d, is freely adjusted in the range of 1–11 mm to control the number

Y.F. Chen (✉) · Y.J. Huang · P.Y. Chiang · Y.C. Lin · H.C. Liang
Department of Electrophysics, National Chiao Tung University,
1001 TA Hsueh Road, Hsinchu 30050, Taiwan
e-mail: yfchen@cc.nctu.edu.tw
Fax: +886-35-725230

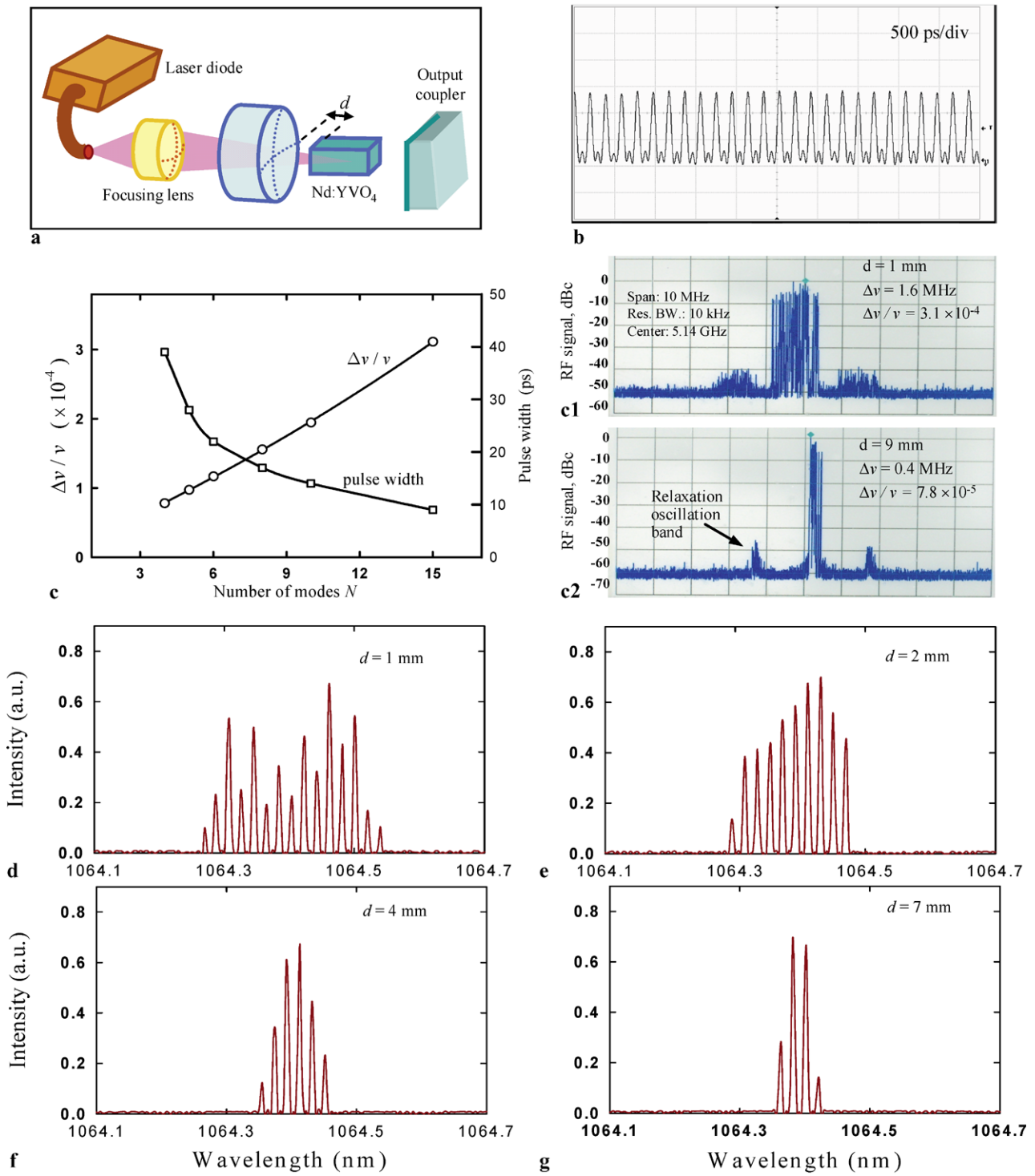

Fig. 1 (**a**) Cavity configuration. (**b**) Typical mode-locked pulse train. (**c**) Relative frequency deviation of the power spectra $\Delta\nu/\nu$ and pulse width versus number of longitudinal lasing modes. (**c1**) and (**c2**) Images of the measured RF power spectra for the cases of $d = 1$ mm and $d = 9$. (**d**)–(**g**) Experimental optical spectra for different crystal/mirror separations

of longitudinal lasing modes via the SHB effect. The gain medium is a-cut 0.5 at.% Nd:YVO_4 crystal with dimensions of $3 \times 3 \times 6$ mm^3. Both end surfaces of the Nd:YVO_4 crystal were antireflection coated at 1064 nm and wedged 2° to avoid the Fabry–Pérot etalon effect. The laser crystal was wrapped with indium foil and mounted in a water-cooled copper holder. The water temperature was maintained at around 20°C to ensure stable laser output. The input mirror

was a 20-cm radius-of-curvature concave mirror with antireflection coating at 808 nm on the entrance face and with high-reflectance coating at 1064 nm (>99.8%) and high transmittance coating at 808 nm on the second surface. A flat wedged output coupler with 10% transmission at 1064 nm was used throughout the experiment. The pump source was a 3-W 808-nm fiber-coupled laser diode with core diameter of 100 μm and numerical aperture of 0.20. Focusing lens with 25 mm focal length and 85% coupling efficiency was used to reimage the pump beam into the laser crystal. The average pump size was approximately 60 μm. The optical cavity length was set to be approximately 2.92 cm, corresponding to a free spectral range of 5.14 GHz. The mode-locked pulses were detected by a high-speed InGaAs photodetector with rise time 35 ps, whose output signal was connected to a digital oscilloscope (Agilent, DSO 80000) with 12 GHz electrical bandwidth and sampling interval of 25 ps. The output signal of the photodetector was also analyzed by an RF spectrum analyzer (Advantest, R3265A) with bandwidth of 8 GHz. The spectral information of the laser was monitored by a Fourier optical spectrum analyzer (Advantest, Q8347) that is constructed with a Michelson interferometer with resolution of 0.003 nm.

With the optimal alignment for $d = 1$ mm, the laser output had a slope efficiency of 31%; the output power reached 0.79 W at an incident pump power of 2.6 W. With the real-time dynamical temporal trace, the laser cavity can be easily adjusted to be in a SML operation with a pulse repetition rate of 5.14 GHz, as shown Fig. 1(b). We also found that the average output power is nearly independent of the crystal/mirror separation d in the range of 1–11 mm. Figures 1(d)–1(g) depict the measured optical spectra. The number of longitudinal lasing modes can be clearly seen to decrease with increasing the separation d. We also measured the radio-frequency (RF) spectrum of the output power to evaluate the stability of mode-locked pulse train. Figure 1(c) shows the experimental results for the relative frequency deviation of the power spectra, $\Delta\nu/\upsilon$, where υ is the center frequency of the power spectrum and $\Delta\nu$ is the frequency deviation of full width at half maximum and is inferred from the beat note spectrum. As shown in Fig. 1(c), the value of $\Delta\nu/\upsilon$ is significantly reduced with decreasing the number of longitudinal lasing modes. Figures 1(c1) and 1(c2) are the images of the measured RF power spectra for the cases of $d = 1$ mm and $d = 9$ mm, respectively. It can be seen that the relaxation oscillation sidebands is improved approximately from −40 dBc to −50 dBc. Since the relaxation oscillation frequencies for different lasing modes are somewhat different, the decrease of the number of lasing modes is found to be beneficial in reducing the frequency deviation for the mode-locked oscillation. The influence of the relaxation oscillation on the dynamics of multimode Nd-doped lasers can be referred to [17–19]. The pulse width was measured with the help of the commercial autocorrelator (APE pulse check, Angewandte physik & Elektronik GmbH) and assuming the sech^2-shaped temporal profile. As depicted in Fig. 1(c), the pulse width increases from 9 ps to 39 ps for the separation d being varied from 1 mm to 11 mm. The mode-locked pulses are nearly bandwidth-limited. Our experimental results manifestly reveal that the compromise between pulse stability and pulse width should be considered in designing an appropriate SML laser.

3 Theoretical analysis for number of lasing modes

Since the number of longitudinal modes play a critical role for the stability of the SML operation, it is useful to develop a method for estimating the number of lasing modes. Here we extend the early work of Zayhowski [16] to derive an analytical formula for estimating the maximum number of longitudinal modes in terms of the cavity geometry and well-known material parameters. Considering a standing-wave laser consisting of N oscillating modes and presuming that all modes have equal amplitude and phase, the normalized electric field can be given by

$$E_N(x,y,z,t) = \left[\frac{1}{\sqrt{N}}\sum_{m=0}^{N-1} e^{i\omega_m t}\sqrt{\frac{2}{l_{\mathrm{cav}}}}\sin(k_m z)\right]\psi(x,y,z), \tag{1}$$

where $\omega_m = (m_o + m)\pi c/l_{\mathrm{cav}}$, $k_m = \omega_m/c$, m_o is the resonant mode index, and l_{cav} is the effective cavity length. The transverse wave function $\psi(x,y,z)$ is given by

$$\psi(x,y,z) = \sqrt{2/\pi w_l^2}\exp\left[-\left(x^2+y^2\right)/w_l^2\right], \tag{2}$$

where w_l is the beam radius. Since the cavity length is much longer than the laser wavelength, the typical value of m_o is greater than 10^3. Thus always $N \ll m_o$ holds. After some algebra, the intensity $I_N(x,y,z,t) = |E_N(x,y,z,t)|^2$ can be expressed as

$$\begin{aligned} I_N(x,y,z,t) &= N/(2l_{\mathrm{cav}})\left\{\left[S_N\left(\pi(ct+z)/(2l_{\mathrm{cav}})\right)\right]^2\right. \\ &\quad + \left[S_N\left(\pi(ct-z)/(2l_{\mathrm{cav}})\right)\right]^2 \\ &\quad - 2S_N\left(\pi(ct+z)/(2l_{\mathrm{cav}})\right)S_N\left(\pi(ct-z)/(2l_{\mathrm{cav}})\right) \\ &\quad \left.\times\cos(2kz)\right\}\left|\psi(x,y,z)\right|^2, \end{aligned} \tag{3}$$

where $S_N(\theta) = \sin(N\theta)/N\sin\theta$ and $k = [m_o + (N-1)/2]\pi/l_{\mathrm{cav}} \approx \omega_o/c$. The intensity $I_N(x,y,z,t)$, averaged

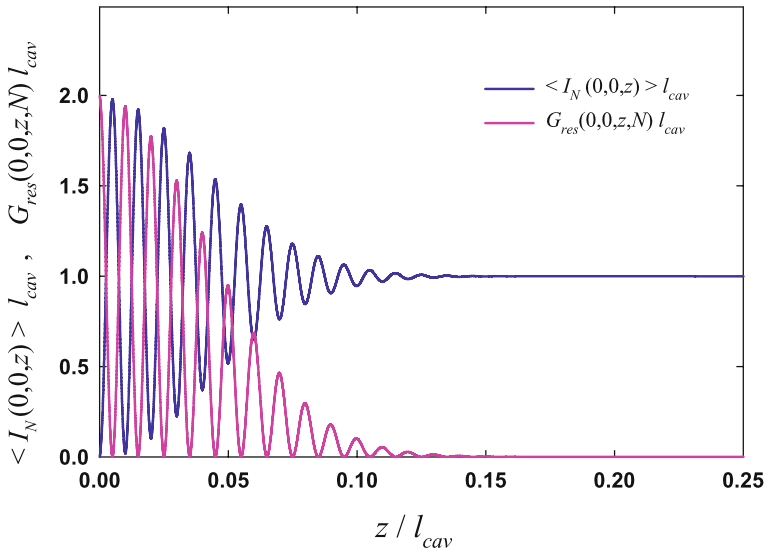

Fig. 2 Calculated results for $G_{res}(x, y, z; N)$ (*pink line*) and $\langle I_N(x, y, z)\rangle$ (*blue line*) as functions of z with $N = 11, x = y = 0$, and $m_o = 200$

over an round trip time $T = 2l_{\rm cav}/c$, becomes

$$\begin{aligned}&\big\langle I_N(x, y, z)\big\rangle\\ &\quad = (1/l_{\rm cav})\big[1 + S_N(\pi z/l_{\rm cav}) - 2S_N(\pi z/l_{\rm cav})\cos^2(kz)\big]\\ &\qquad \times \big|\psi(x, y, z)\big|^2. \end{aligned} \tag{4}$$

The function represents a standing-wave pattern which is fully modulated for the position near the reflecting mirrors and continuously loses contrast for the position away from the mirrors. Due to the standing-wave nature, superposition of the light fields of modes results in an envelope function for the total light intensity. The spatial variation of the envelope $S_N(\pi z/l_{\rm cav})$ occurs on the cavity-length scale to be much slower compared to rapid undulations of the intensities of individual modes. As N get larger, $S_N(\pi z/l_{\rm cav})$ becomes narrower such that it only has weight very close to the end mirrors, i.e., $z = 0$ and $z = l_{\rm cav}$. The envelope function $S_N(\pi z/l_{\rm cav})$ has a damping oscillation in the tail, causing some inconvenience in performing numerical integration. For a convenient numerical evaluation we use a Gaussian function

$$g_N(z) = e^{-[N\pi z/2l_{\rm cav}]^2} + e^{-[N\pi(l_{\rm cav}-z)/2l_{\rm cav}]^2} \tag{5}$$

to replace the envelope function $S_N(\pi z/l_{\rm cav})$. In terms of $g_N(z)$, the average intensity in (4) can be split into two terms:

$$\begin{aligned}&\big\langle I_N(x, y, z)\big\rangle\\ &\quad = \big|\psi(x, y, z)\big|^2\big[1 + g_N(z)\big]/l_{\rm cav} - G_{\rm res}(x, y, z; N), \end{aligned} \tag{6}$$

where the first term $|\psi(x, y, z)|^2[1 + g_N(z)]/l_{\rm cav}$ indicates the average intensity without the interference effect and the second term

$$G_{\rm res}(x, y, z; N) = (2/l_{\rm cav})\cos^2(kz)g_N(z)\big|\psi(x, y, z)\big|^2 \tag{7}$$

represents the residual gain distribution due to the interference term $\cos^2(kz)$ of the SHB effect. Figure 2 depicts the calculated results for $G_{\rm res}(x, y, z; N)$ and $\langle I_N(x, y, z)\rangle$ as functions of z, where we take $N = 11, x = y = 0$, and $m_o = 200$ for the convenience of presentation.

The maximum number of modes $N_{\rm max}$ that can oscillate in a standing-wave cavity is determined from the condition that the maximum value of N in $G_{\rm res}(x, y, z; N)$ leads to the effective round-trip gain not less than the round-trip losses, i.e.,

$$\begin{aligned}&2\sigma l_g(P_{\rm abs}\tau/h\upsilon_p)\\ &\qquad \times \iiint G_{\rm res}(x, y, z, N)r_p(x, y, z)\, dV\Big|_{N=N_{\rm max}}\\ &\quad \geq \ln(1/R) + L, \end{aligned} \tag{8}$$

where σ is the stimulated emission cross section, l_g is the length of the gain medium, $P_{\rm abs}$ is the absorbed pump power, υ_p is the pump frequency, τ is the emission lifetime, L is the round-trip loss, R is the reflectivity of the output coupler, and $r_p(x, y, z)$ is the normalized pump intensity distribution. For a gain medium located between $z = d$ and $z = d + l_g$ and using a circular Gaussian beam to express the pump distribution, $r_p(x, y, z)$ is given by

$$\begin{aligned}&r_p(x, y, z)\\ &\quad = \big(2/\pi w_p^2\big)\big[\alpha e^{-\alpha(z-d)}/\big(1 - e^{-\alpha l_g}\big)\big]e^{-2(x^2+y^2)/w_p^2}\\ &\qquad \times \Theta(z - d)\Theta(d + l_g - z), \end{aligned} \tag{9}$$

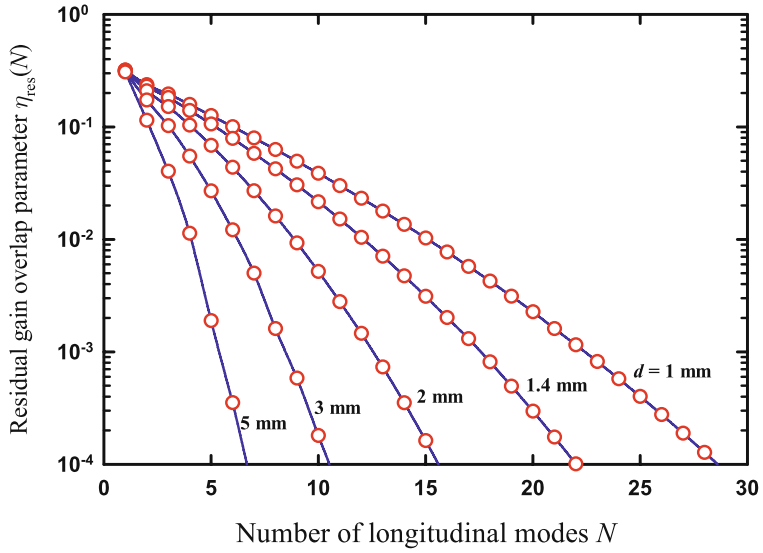

Fig. 3 Calculated results for $\eta_{\mathrm{res}}(N, d)$ as a function of N for several different values of d for the case of the Nd:YVO_4 laser

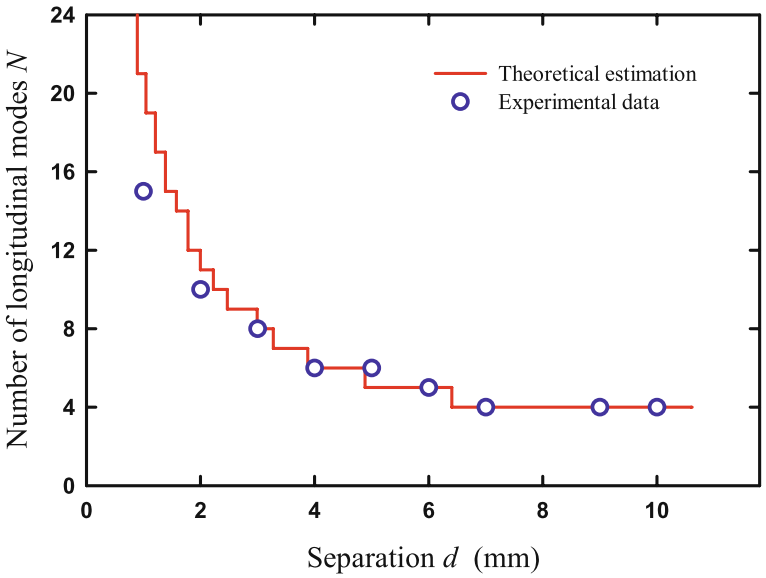

Fig. 4 Theoretical estimations and experimental data for the maximum number of modes $N_{\max}$ as a function of d

where α is the absorption coefficient at the pump wavelength, w_p is the pump radius, and $\Theta(\,)$ is the Heaviside step function. Note that the gain saturation effect is neglected because of low intensity levels. Substituting (7) and (9) into (8) and carrying out the integration in the transverse directions, we can obtain the relationship of $\eta_{\mathrm{res}}(N, d)|_{N=N_{\max}} \geq \zeta$, where the residual gain overlap parameter $\eta_{\mathrm{res}}(N, d)$ is defined as

$$\eta_{\mathrm{res}}(N, d) = (2/l_{\mathrm{cav}})\left[\alpha l_g/\left(1 - e^{-\alpha l_g}\right)\right] \times \int_d^{d+l_g} \cos^2(kz) g_N(z) e^{-\alpha(z-d)}\, dz \tag{10}$$

and the effective loss-to-pump factor ζ is defined as

$$\zeta = \frac{[\ln(1/R) + L]}{(I_p/I_s)}, \tag{11}$$

where $I_p = 2P_{\mathrm{abs}}/[\pi(w_l^2 + w_p^2)]$ and $I_s = h\upsilon_p/(\sigma\tau)$. The residual gain overlap parameter $\eta_{\mathrm{res}}(N, d)$ represents the overlap efficiency between the residual gain distribution and the pump absorption distribution in the longitudinal direction. The effective loss-to-pump factor ζ indicates the ratio of the cavity loss $\ln(1/R) + L$ to the transverse gain coefficient I_p/I_s. As a result, the maximum number of modes $N_{\max}$ can be determined with the criterion $\eta_{\mathrm{res}}(N, d)|_{N=N_{\max}} \geq \zeta$ and (10) and (11). Figure 3 shows the calculated results for $\eta_{\mathrm{res}}(N, d)$ as a function of N for several different values of d for the case of the Nd:YVO_4 laser: $l_{\mathrm{cav}} = 29$ mm, $l_g = 6$ mm, and $\alpha = 0.5$ mm^{-1}. From Fig. 3, it is clear that the maximum number of modes $N_{\max}$ is decreased with increasing d. For the experimental condition in Fig. 1, the effective loss-to-pump factor ζ can be found to be 3.1×10^{-3}, where the values of the parameters are as

follows: $\sigma = 2.5 \times 10^{-18}$ cm^2, $P_{\text{abs}} = 2.5$ W, $\tau = 100$ μs, $R = 0.9$, $L = 0.005$, $hv_p = 2.45 \times 10^{-19}$ J, $w_l = 0.06$ mm, and $w_p = 0.06$ mm. Applying $\zeta = 3.1 \times 10^{-3}$ into Fig. 3, the maximum number of modes N_{max} can be determined as a function of d, as depicted in Fig. 4. The good agreement between the theoretical estimations and the experimental data validate the usefulness of the present model.

4 Conclusions

In conclusion, we have experimentally confirmed that a SML can occur in short-cavity Nd:YVO_4 lasers without employing an extra nonlinearity. We further found that the stability of the SML pulses could be significantly improved by reducing the number of longitudinal lasing modes to diminish the phase fluctuation. Considering the SHB effect, we have derived an analytical formula to establish the relationship between the number of longitudinal lasing modes and the crystal/mirror separation. The theoretical estimations for the number of longitudinal lasing modes were shown to be in good agreement with experimental observations.

Acknowledgement This work is supported by the National Science Council of Taiwan (Contract No. NSC-97-2112-M-009-016-MY3).

References

1. M.H. Crowell, IEEE J. Quantum Electron. **1**, 12 (1965)
2. H. Statz, C.L. Tang, J. Appl. Phys. **36**, 3923 (1965)
3. M.A. Duguay, S.L. Shapiro, P.M. Rentzepis, Phys. Rev. Lett. **19**, 1014 (1967)
4. O.L. Gaddy, E.M. Schaefer, Appl. Phys. Lett. **9**, 281 (1966)
5. H.C. Liang, R.C.C. Chen, Y.J. Huang, K.W. Su, Y.F. Chen, Opt. Express **16**, 21149 (2008)
6. P. Glas, M. Naumann, A. Schirrmacher, L. Däweritz, R. Hey, Opt. Commun. **161**, 345 (1999)
7. A.A. Grütter, H.P. Weber, R. Dändliker, Phys. Rev. **185**, 629 (1969)
8. R. Dändliker, A.A. Grütter, H.P. Weber, IEEE J. Quantum Electron. **6**, 687 (1970)
9. H. Statz, J. Appl. Phys. **38**, 4648 (1967)
10. H. Statz, M. Bass, J. Appl. Phys. **40**, 377 (1969)
11. H. Fu, H. Haken, Phys. Rev. A **43**, 2446 (1991)
12. C.J. Flood, D.R. Walker, H.M. van Driel, Opt. Lett. **20**, 58 (1995)
13. H.S. Kim, S.K. Kim, B.Y. Kim, Opt. Lett. **21**, 1144 (1996)
14. L. Jiang, L.V. Asryan, IEEE Photonics Technol. Lett. **20**, 1661 (2008)
15. G.J. Kintz, T. Baer, IEEE J. Quantum Electron. **26**, 1457 (1990)
16. J.J. Zayhowski, Opt. Lett. **15**, 431 (1990)
17. T. Hill, M.W. Hamilton, D. Pieroux, P. Mandel, Phys. Rev. A **66**, 063803 (2002)
18. B. Peters, J. Hünkemeier, V.M. Baev, Y.I. Khanin, Phys. Rev. A **64**, 023816 (2001)
19. N.B. Abraham, L. Sekaric, L.L. Carson, V. Seccareccia, P.A. Khandokhin, Ya.I. Khanin, I.V. Koryukin, V.G. Zhislina, Phys. Rev. A **62**, 013810 (2000)